

Article

Understanding Penetration Attenuation of Permeable Concrete: A Hybrid Artificial Intelligence Technique Based on Particle Swarm Optimization

Fei Zhu ^{1,2}, Xiangping Wu ^{3,*}, Yijun Lu ⁴ and Jiandong Huang ^{4,*}¹ School of Fine Arts, Suzhou Vocational University, Suzhou 215104, China; zhufeiedu@163.com² School of Civil Engineering, China University of Mining and Technology, Xuzhou 221116, China³ Department of Gem Design Engineering, KAYA University, Gimhae 50830, Republic of Korea⁴ School of Civil Engineering, Guangzhou University, Guangzhou 511370, China; yijun.lu@e.gzhu.edu.cn

* Correspondence: xiangping_wu@163.com (X.W.); jiandong.huang@hotmail.com (J.H.)

Abstract: Permeable concrete is a type of porous concrete with the special function of water permeability, but the permeability of permeable concrete will decrease gradually due to the clogging behavior arising from the surrounding environment. To reliably characterize the clogging behavior of permeable concrete, particle swarm optimization (PSO) and random forest (RF) hybrid artificial intelligence techniques were developed in this study to predict the permeability coefficient of permeable concrete and optimize the aggregate mix ratio of permeable concrete. Firstly, a reliable database was collected and established to characterize the input and output variables for the machine learning. Then, PSO and 10-fold cross-validation were used to optimize the hyperparameters of the RF model using the training and testing datasets. Finally, the accuracy of the developed model was verified by comparing the predicted value with the actual value of the permeability coefficients ($R = 0.978$ and $RMSE = 1.3638$ for the training dataset; $R = 0.9734$ and $RMSE = 2.3246$ for the testing dataset). The proposed model can provide reliable predictions of the clogging behavior that permeable concrete may face and the trend of its development.

Keywords: permeable concrete; PSO; RF; water permeability; hybrid artificial intelligence techniques



Citation: Zhu, F.; Wu, X.; Lu, Y.; Huang, J. Understanding Penetration Attenuation of Permeable Concrete: A Hybrid Artificial Intelligence Technique Based on Particle Swarm Optimization. *Buildings* **2024**, *14*, 1173. <https://doi.org/10.3390/buildings14041173>

Academic Editor: Alireza Entezami

Received: 29 December 2023

Revised: 28 February 2024

Accepted: 1 April 2024

Published: 21 April 2024



Copyright: © 2024 by the authors. Licensee MDPI, Basel, Switzerland. This article is an open access article distributed under the terms and conditions of the Creative Commons Attribution (CC BY) license (<https://creativecommons.org/licenses/by/4.0/>).

1. Introduction

The traditional concrete structure is dense, and rainwater does not easily pass through, so it is easy to observe urban waterlogging in the season of heavy rainfall [1,2]. At the same time, groundwater cannot be replenished in time; therefore, groundwater resources have gradually decreased. Permeable concrete is a type of functional concrete that prevents water accumulation on the ground by artificially setting gaps in the concrete, so that the surface water can pass through freely [3,4]. During the preparation of permeable concrete, the interspaces of concrete can be connected by adopting corresponding technical measures [5,6]. Permeable concrete refers to the concrete with internal porosity that is greater than 10%, generally 15% to 30%, and most of the pore diameters are greater than 1 mm, with certain water and air permeability [7–11]. As the organic matter and fine-grained impurities block the voids of the permeable concrete, water permeability becomes an urgent problem to be solved in the application [7,12,13]. Impurities, such as leaves, pine needles, nuts, sprouts, grass clippings, soil washed away by runoff, and sand falling from the concrete, can all become the components to block permeable concrete [8]. Also, industrial experience has shown that even if there is no organic matter and fine-grained materials directly invading the permeable concrete, the permeability will still decrease over time [14] (as shown in Figure 1).

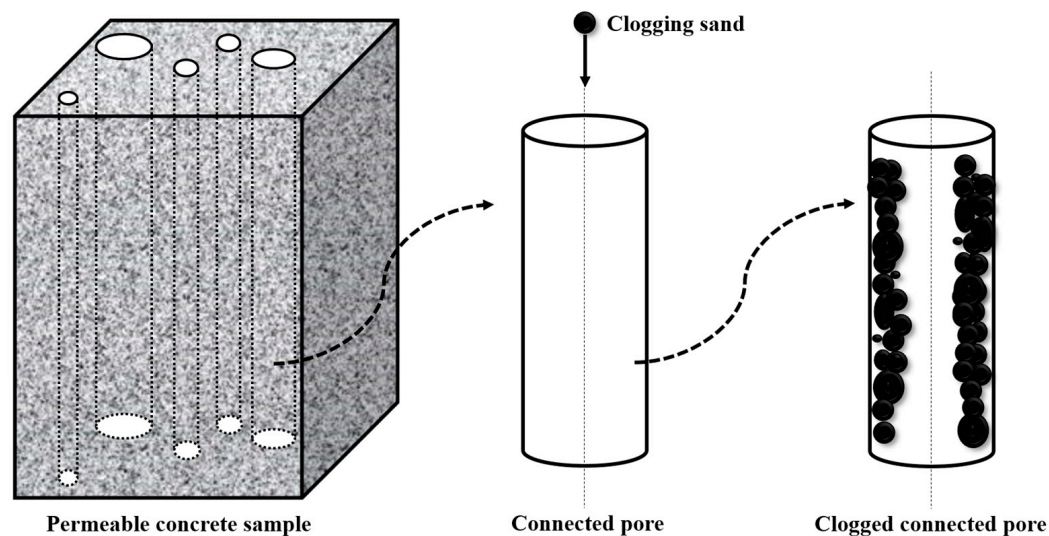


Figure 1. Penetration attenuation of permeable concrete.

Observing the obstructions in the voids of permeable concrete, it is found that they are composed of fine sand particles and squeezed organic matter [15]. These obstructions generally cluster together in the voids of permeable concrete [16]. The obstructions in the voids of permeable concrete pavement will decompose or re-synthesize over time, which will affect the permeability of permeable concrete. Therefore, the agglomeration of obstructions is regarded as the main factor determining the permeability of permeable concrete [7,17–19].

Permeable concrete is a functional concrete that is used in cities to realize the ecological circulation of water resources and improve the natural ecological environment [20]. The proposal of “sponge city” has increased the attention to the application of permeable concrete research. Permeable concrete is a type of multi-void concrete with high porosity; therefore, its mechanical properties, such as compressive strength, are poor, and it is often used in urban streets, residential parks, and other areas with high requirements for road permeability [21]. The permeable effect of permeable concrete is related to the service environment, the material properties of permeable concrete, and cleaning and maintenance methods [22,23]. The permeability of permeable concrete varies with rainfall, topography, and the proportion of blocked particles [24]. In terms of material properties, the permeability effect of permeable concrete is mainly related to the water–cement ratio, the porosity, the thickness of the concrete specimen, and the aggregate diameter [25]. The blocked particles trapped in the surface of permeable concrete are the main factors leading to the decrease in the permeability of permeable concrete. Timely cleaning and maintenance of permeable concrete are beneficial to reducing the decline of the permeability of permeable concrete [26]. To improve the permeability of permeable concrete, it is of great significance to study the composition materials of permeable concrete.

Researchers often use the laboratory test method to study the performance of concrete, but this method not only has the disadvantage of low efficiency but also requires a lot of money [27]. To solve the inevitable shortcomings of the laboratory experiment method, some researchers have proposed to use artificial intelligence models for the regression prediction [28–45], such as multilayer perceptron (MLP), feed-forward (FF), radial basis function (RBF), and recurrent neural networks (RNN). Zhang et al. studied random forests (RF), support vector machine (SVM), and artificial neural network (ANN) models to solve the complex fatigue problems of concrete materials, and proposed a strength degradation model for evaluating the residual strength of concrete under fatigue loads [46]. Imran et al. developed a multiple regression (MPR) model to predict the compressive strength of eco-friendly concrete and compared the prediction performance of this model with the linear regression (LR) model and the SVM model. The results showed that the prediction

performance of the new model was superior to the other two models [47]. Han et al. proposed a method for predicting the elastic modulus of concrete containing recycled aggregate and compared the prediction effect of the integrated learning model with that of five commonly used artificial intelligence models. The results showed that the prediction effect of the elastic modulus of concrete containing recycled aggregate was better than that of the single artificial intelligence model [48]. Liu et al. studied the different artificial intelligence models for the prediction of the recycled aggregate concrete carbonation depth effect. The results showed that the predicted effect of the RF model was better than the gaussian process regression (GPR) model and independent of the ANN model [49]. All the above artificial intelligence models have achieved good results in predicting concrete performance, indicating that artificial intelligence techniques have broad prospects in predicting concrete performance [50,51]. Although the permeable effect of permeable concrete is facing great problems, which need to be solved urgently, there are few types of research on the water permeability of permeable concrete using the artificial intelligence method. Also, to the knowledge of the authors, the thickness of permeable pavement has not been considered in the prediction of the clogging behavior of permeable concrete.

To effectively simulate the clogging behavior of permeable concrete and reduce the cost of numerous laboratory tests, a numerical simulation study was carried out. In addition, to improve the reliability of the modeling, a hybrid artificial intelligence technique was developed to predict and simulate the clogging behavior of permeable concrete under different clogging particles. The proposed study provides a theoretical basis for subsequent researchers to study the clogging behavior of permeable concrete.

2. Research Aims

The main aim of this research was to evaluate and model the clogging behavior of permeable concrete by predicting the permeability coefficient using machine learning techniques, intending to understand the clogging behavior of permeable concrete and the trend of its development. A hybrid AI algorithm combining the PSO and RF models is proposed to improve the efficiency and accuracy of the prediction process. The permeable concrete was mixed and designed using four types of aggregates (2.36–4.75 mm, 4.75–9.50 mm, 9.50–16.0 mm, and 16.0–19.0 mm). The input parameters were determined as the different proportions of these four types of aggregates. To consider the permeable pavement thickness, the sample thicknesses were determined as 50 mm, 100 mm, and 150 mm, respectively. The permeability reduction tests were conducted using three types of clogging sands of different sizes (0–0.25 mm, 0.25–0.5 mm, and 0.5–1 mm). After the laboratory tests, the hybrid model based on the PSO-RF algorithm was employed to construct a hybrid artificial intelligence technique to predict the permeability under varying clogging sands. Figure 2 presents the research process of this study.

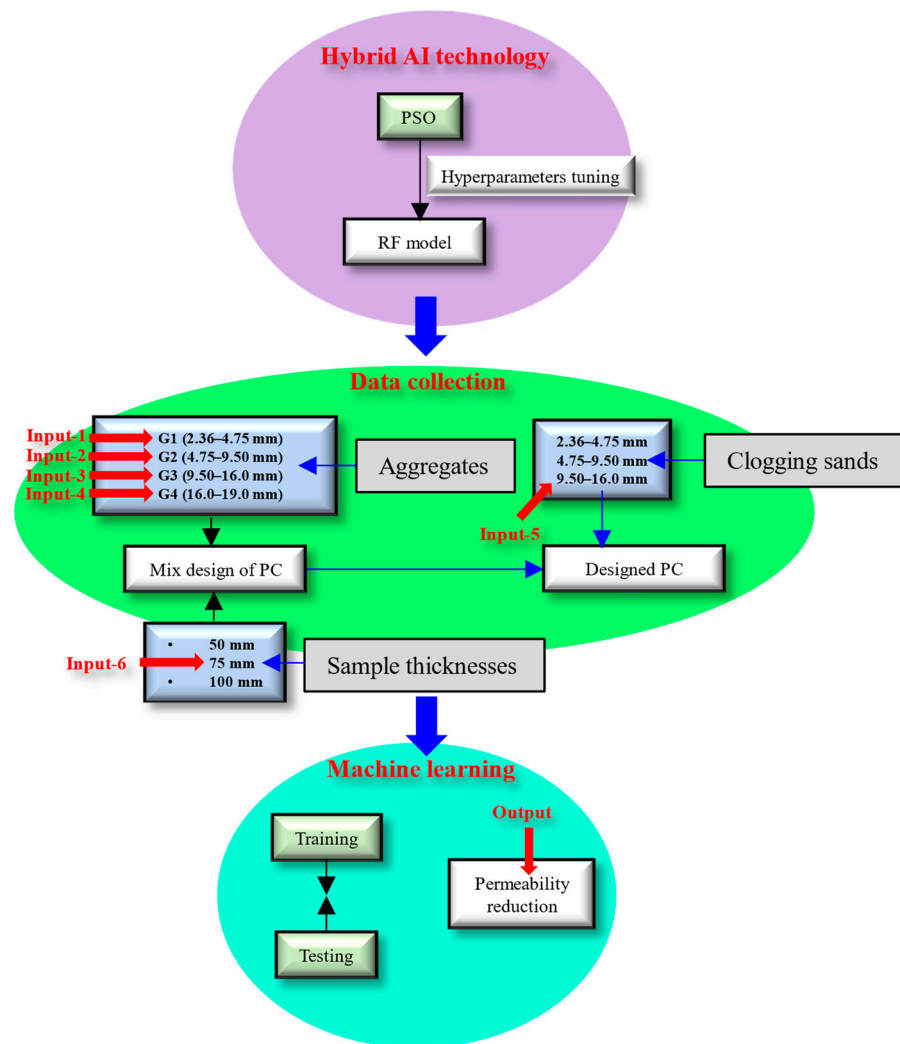


Figure 2. Flow chart of the research process.

3. Data Collection

The employment of machine learning techniques to predict the performance of concrete is a recent research hotspot. Researchers are eager to develop novel and effective artificial intelligence techniques for predicting concrete performance, but often ignore the importance of a database for verifying the prediction effect of the model on concrete performance. To more accurately verify the prediction effect of the PSO and RF hybrid artificial intelligence techniques developed in this study on the permeability of permeable concrete, this study established a reliable database based on the dataset collected from previous studies [52]. Compared with another algorithm for hyperparameter tuning, the PSO algorithm has no crossover and mutation operations and relies on particle speed to complete the search. Moreover, in the iterative evolution, only the optimal particle transmits information to the other particles, and the search speed is fast. There are also fewer parameters to be adjusted; therefore, the structure is simple, and it is easy to predict the clogging behavior of permeable concrete. In the database employed in this study, the proportion of four aggregates (2.36–4.75 mm, 4.75–9.50 mm, 9.50–16.0 mm, and 16.0–19.0 mm), the thickness of three different concrete specimens (0–0.25 mm, 0.25–0.5 mm, and 0.5–1 mm), and three different sizes of blocking sand (0–0.25 mm, 0.25–0.5 mm, and 0.5–1 mm) were regarded as input variables. The datasets of 84 groups (as shown in the appendix) were randomly divided into two parts, one of which accounted for 70% of the total dataset as the training set, and the other accounted for 30% of the total dataset as the test set.

4. Methodology

4.1. Random Forest (RF) Model

The RF model combines multiple weak classifiers, and the final results are voted or averaged so that the results of the overall model have high accuracy and generalization performance. The good performance of the model is mainly due to “randomness” and “forest”, one making it resistant to overfitting, the other making it more accurate. A random forest is made up of many classifications and regression trees (CART), and there is no correlation between the different carts. As the classification task is carried out, new input samples will enter and each decision tree in the forest will be allowed to judge and classify separately. Each decision tree will have its own classification result; the random forest will take the classification results of the decision tree that has the most classification as the final result.

4.1.1. Classification and Regression Tree (CART)

CART uses binary recursive segmentation to divide the original sample set into two subsets so that there will be two branches on each non-leaf node. In the case of node splitting, the splitting rule follows the minimum principle of the Gini index, and the probability distribution of the Gini index can be calculated using [53,54]:

$$Gini(p) = \sum_{k=1}^K p_k(1 - p_k) = 1 - \sum_{k=1}^K p_k^2 \quad (1)$$

where K is the total number of feature samples in the node, and p_k is the probability of the feature samples of class K in the node. The Gini index of one dataset can be determined as follows:

$$Gini(D) = 1 - \sum_{k=1}^K \left(\frac{|C_k|}{|D|} \right)^2 \quad (2)$$

The Gini index divided by each node can be calculated using the following equation:

$$Gini_{split}(D) = \frac{|D_1|}{|D|} Gini(D_1) + \frac{|D_2|}{|D|} Gini(D_2) \quad (3)$$

where D_1 and D_2 are the two subsets of the permeability dataset.

4.1.2. Bagging Algorithm for the Permeability Coefficients

The bagging algorithm sets a series of weak classifiers into a strong classifier, and each weak classifier classifies and predicts the data on the permeability coefficients independently, which can improve the generalization performance of the classifier and improve the accuracy of the final result. The bagging algorithm is a retractable sampling method, that is, based on repeatable random sampling, each sample is obtained using the retractable sampling of the initial dataset of the permeability coefficients. The bootstrap method (Figure 3) was used to randomly select the N training samples of the permeable concrete (pc1, pc2, pc3) from the original sample set, and the process was carried out for N tree cycles to obtain the N tree training sets, which were independent of each other.

According to the method in Figure 3, the N tree training dataset can generate N tree models. To model the clogging behavior of permeable concrete, the permeability can be determined using the average of the N tree models. The flow chart of the bagging algorithm is summarized in Figure 4.

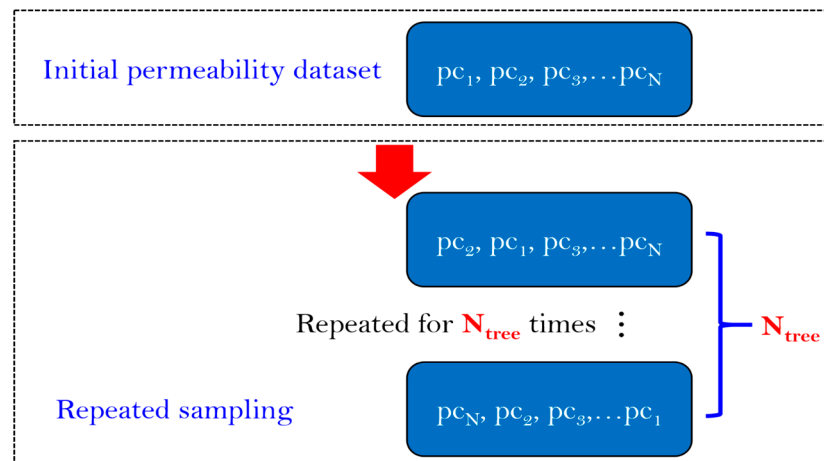


Figure 3. Bootstrap method.

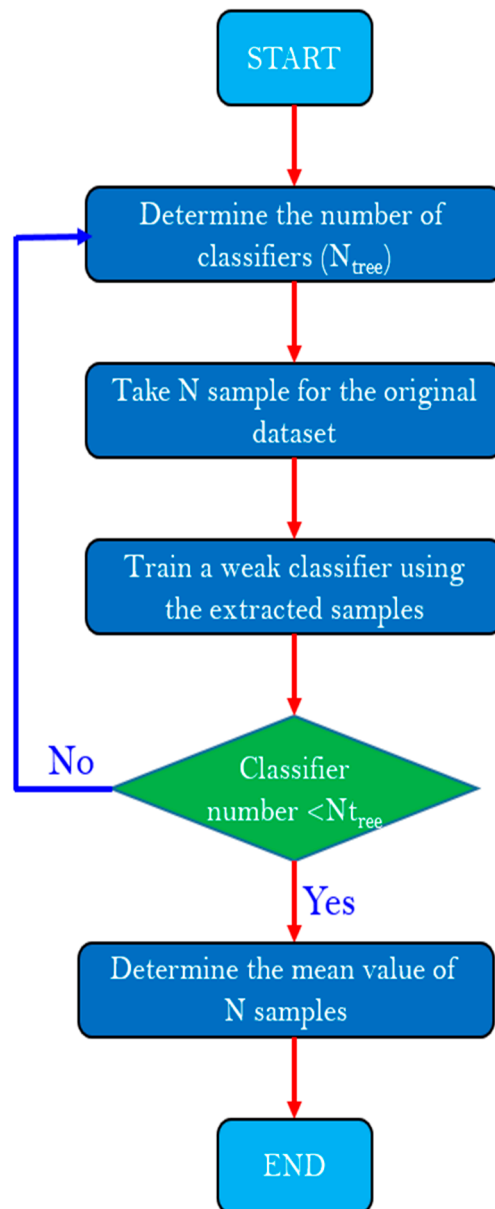


Figure 4. Flow chart of the bagging algorithm.

4.1.3. RF Modeling for the Permeability Prediction

The construction of the RF algorithm consists of three stages: training set generation, decision tree construction, and algorithm formation. First, the bagging algorithm is used to generate the n unrelated training sets without placing back sampling randomly. Then, the n training sets are trained separately to build a decision tree. Finally, the N decision trees are integrated to form the RF model. The flow chart used to construct the RF model to predict the clogging behavior of permeable concrete is shown in Figure 5.

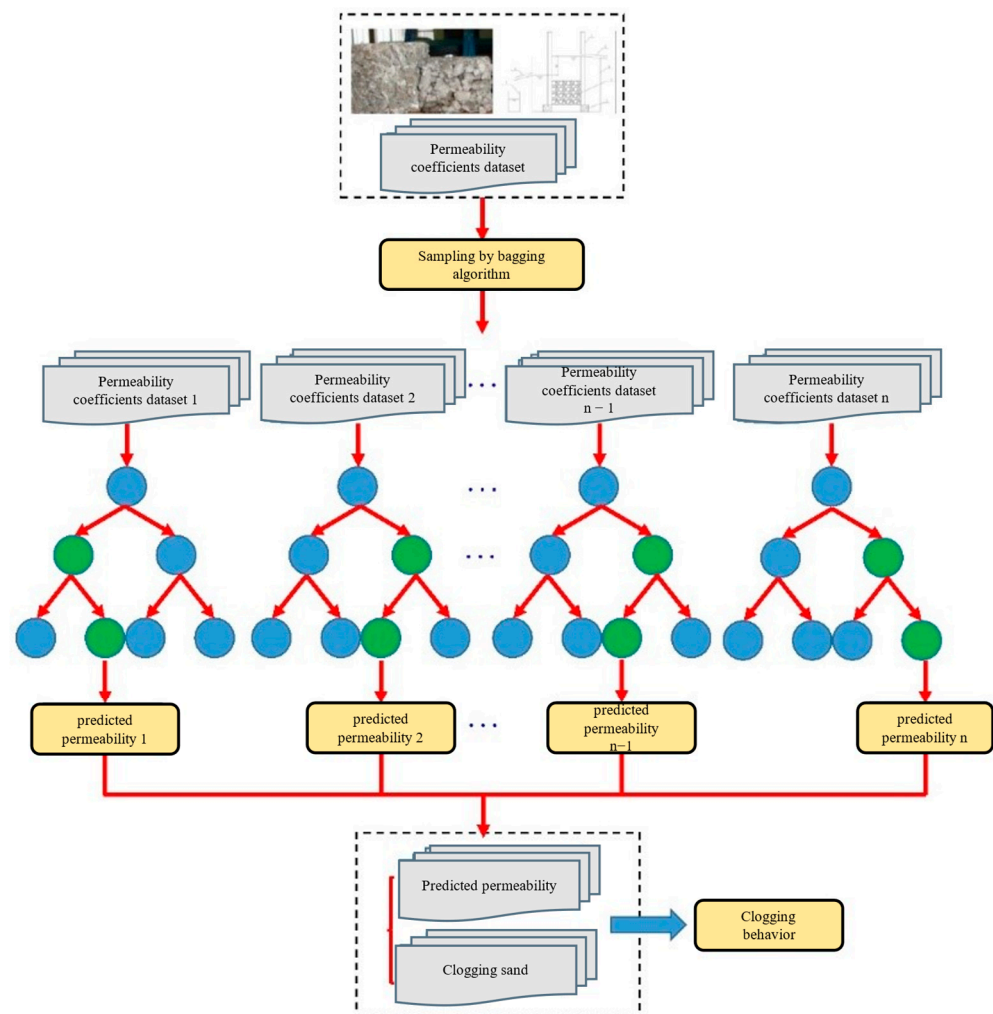


Figure 5. Modeling the clogging behavior using the RF algorithm.

4.2. Random Forest (RF) Model

The PSO algorithm compares the whole particle swarm to a bird flock, and each particle in the population has the attributes of position, speed, and fitness value. A particle represents a feasible solution in the feasible domain of the solution, but it is not necessarily the optimal solution. In addition, each particle does not know the specific location of the target. In each cycle operation, the particle adjusts its own speed and position vector by learning its own historical experience and the historical experience of the population and comparing this with the adaptive value of the previous position to finally achieve the purpose of global optimization.

During the cycle iteration, the velocity and position vectors of the particle were updated as shown below [55,56]:

$$v_{id} = \omega * v_{id} + c_1 * r(x) * (p_{id} - x_{id}) + c_2 * r(x) * (p_{gd} - x_{id}) \quad (4)$$

$$x_{id} = x_{id} + v_{id} \quad (5)$$

where ω is the inertia weight; c_1 and c_2 are the learning factors; and $r(x)$ is the random equation in the range of (0,1). v_{id} should be limited using the following equations:

$$v_{id} = \begin{cases} v_{max}, v_{id} > v_{max} \\ v_{min}, v_{id} < v_{min} \\ v_{id}, v_{min} < v_{id} < v_{max} \end{cases} \quad (6)$$

4.3. Hybrid AI Techniques to Predict the Clogging Behavior

To address the issue that the number of decision trees, n , and the number of splitting features, m , are discrete values in the RF algorithm, the PSO algorithm was used to optimize the parameters of the RF model [57,58]. In detail, the relevant parameters of the RF and PSO algorithms were initialized; the value range, the initial value of the number of decision trees, n , and the splitting feature number, m , in the RF model were given; and the number of iterations in the particle swarm was set. The number of decision trees, n , and the number of splitting features, m , were substituted into the RF model to calculate the average error. The number of iterations was checked to ensure it meets the requirement of the set value and determine the optimized tree number, n_{best} , and splitting characteristic number, m_{best} . In the original dataset of the permeable concrete, the n_{best} training sets were randomly selected using the Bootstrap method to form the n_{best} decision trees. Then, the m_{best} features were randomly selected to form split feature sets. Each decision tree was divided by selecting the optimal split feature until the leaf node. The result of each decision tree was calculated using the arithmetic average value, and the final permeability prediction result of the RF-PSO model was obtained.

4.4. Hyperparameter Tuning

4.4.1. 10-Fold Cross-Validation (CV)

In this research, the 10-fold cross-validation (CV) was used for the hyperparameter tuning in the RF model [59,60]. In the 10-fold CV, the permeability coefficient dataset was divided into 10 subsets, of which 9 subsets were used for the training process and 1 subset was used to validate the permeability prediction results. For the subset used to validate the prediction, the minimum RMSE needs to be determined after 50 iterations to represent the optimal structure of this RF model [61,62]. In other words, such a verification process needs to use the PSO algorithm 50 times to attain the hyperparameters of the RF model. The permeability prediction results should be compared with the clogging behavior model, considering the size of the clogging sand.

4.4.2. Determination of the Prediction Effect

This research applied two parameters (RMSE, root-mean-square error; R, correlation coefficient) to validate the model and evaluate the prediction effect of the model established in this study. The RMSE was defined using the following formula [63,64]:

$$RMSE = \sqrt{\frac{1}{n} \sum_{i=1}^n (y_i^* - y_i)^2} \quad (7)$$

where y_i^* is the predicted permeability coefficient of the permeable concrete; y_i is the measured value of the permeability coefficient of the permeable concrete; n is the number of the permeable concrete samples to conduct the tests of permeability. R was determined using the formula as follows:

$$R = \frac{\sum_{i=1}^n (y_i^* - \bar{y}^*)(y_i - \bar{y})}{\sqrt{\sum_{i=1}^n (y_i^* - \bar{y}^*)^2} \sqrt{\sum_{i=1}^n (y_i - \bar{y})^2}} \quad (8)$$

where y_i^* and y_i are the permeability coefficients of the permeable concrete using the prediction and the measurement, respectively.

5. Results and Discussion

5.1. Analysis of the Permeability Results

This study applied the Pearson correlation coefficient to calculate the relationship between the input parameters that determine the permeability results. The higher the correlation value, the stronger the correlation between the two parameters. When the correlation coefficient between the two parameters is closer to 1, this indicates that the correlation is stronger. Conversely, when the correlation coefficient between the two parameters is closer to 0, this indicates that the correlation is weaker. Figure 6 shows the correlation matrix of the different input parameters, including the proportions of G1, G2, G3, and G4, as well as the sample thickness and clogging sand sizes.

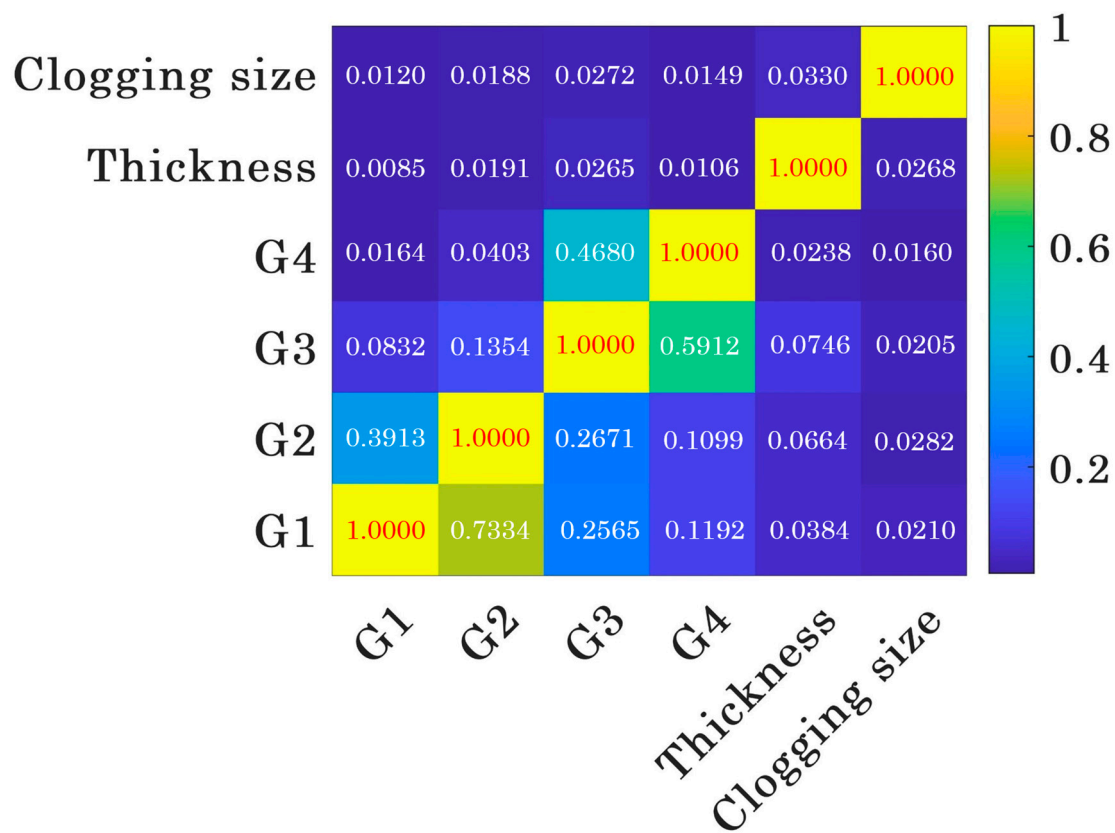


Figure 6. Correlation coefficient analysis.

It can be observed in Figure 6 that the correlation coefficient of the two identical variables on the diagonal is 1 from the bottom left to the top right, and the correlation coefficient of the upper part of the diagonal is symmetrical with that of the lower part of the diagonal. The correlation coefficients between the variables are relatively low (most values are below 0.5). This demonstrates that these input variables are independent of each other and can be used as input variables to predict the clogging behavior of permeable concrete samples without causing multicollinearity problems.

To determine the relationship between input variables and the permeability of permeable concrete, the sensitivity of the input variables and the permeability of permeable concrete were analyzed in this study. Figure 7 presents the sensitive analysis of different input variables.

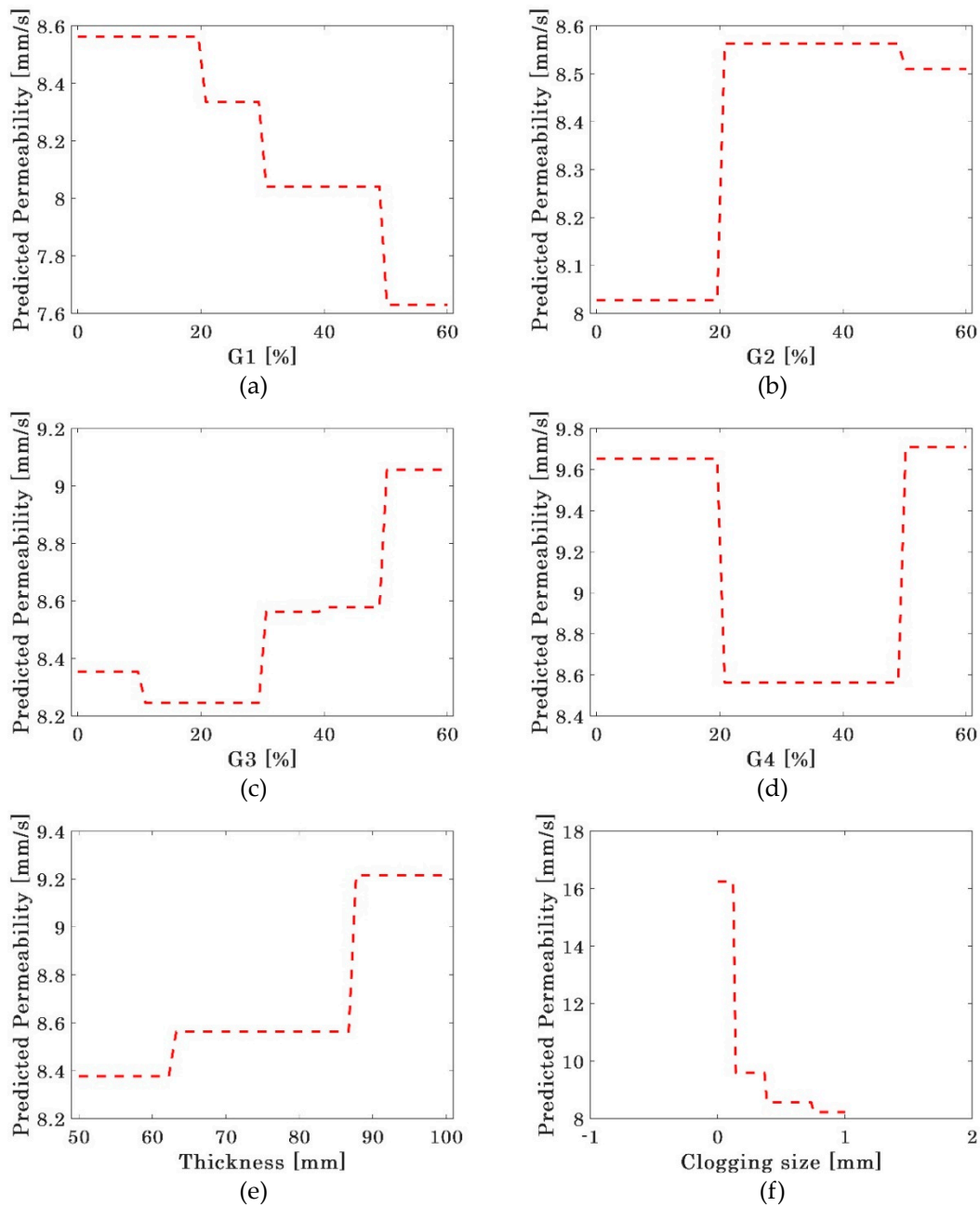


Figure 7. Sensitive analysis of different input variables: (a) proportion of G1 aggregate; (b) proportion of G1 aggregate; (c) proportion of G1 aggregate; (d) proportion of G1 aggregate; (e) sample thickness; (f) clogging sand sizes.

As observed in Figure 7, the proportion of the G1 aggregate is negatively correlated with the permeability coefficient (see Figure 7a), indicating that the aggregate with a small particle size is not conducive to the permeability of permeable concrete. This is because the aggregate size is small and easily filled into the skeleton structure, reducing the voids. For the G2, G3, and G4 aggregates, the influence of the aggregate ratio on the permeability coefficient is relatively random (Figure 7b–d). It can be seen from Figure 7e that the sample thickness is beneficial to the permeability of permeable concrete. This may be because there are more seepage paths in the thicker concrete specimens, increasing the permeability coefficient. It can be seen in Figure 7f that the size of the clogging sand has little influence on the permeability coefficient. The permeability coefficient of permeable concrete can be significantly reduced with larger clogging sand.

5.2. Results of the Hyperparameter Tuning

The hyperparameter of the optimized RF model to predict the permeability was tuned using the 10-fold cross-validation method in this study. In the 10-fold cross-validation method, one subset of the permeability dataset needs to be isolated for the final evaluation of the model. The remaining permeability coefficient data are divided into 10 folded subsets. These folded subsets are then cross-validated iteratively, using one subset as the validation set in each iteration and using all the remaining subsets as the training set. The RMSE values obtained during this process were used for the validation. Figure 8 shows the RMSE values regarding the different fold numbers after the 10-fold cross-validation.

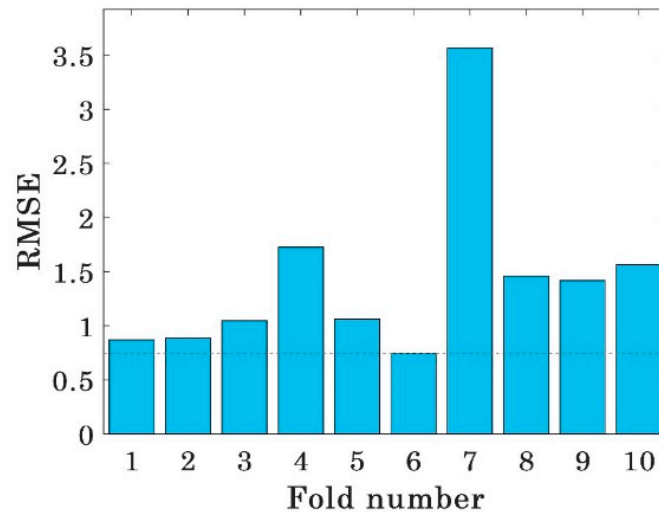


Figure 8. RMSE values for different fold numbers.

As shown in Figure 7, the minimum value of the RMSE can be obtained at the sixth fold from the permeability dataset of the permeable concrete, and the minimum RMSE value is 0.75 mm/s. Therefore, the hyperparameter obtained at the sixth fold was used in the present study to construct the optimized RF model to predict the permeability of permeable concrete.

Figure 9 shows the development of the RMSE values with the increase in the iteration times and demonstrates that the RMSE values can decrease quickly with the increase in the iteration times. It is evident that the PSO algorithm can tune the RF model to predict the permeability of the permeable concrete efficiently.

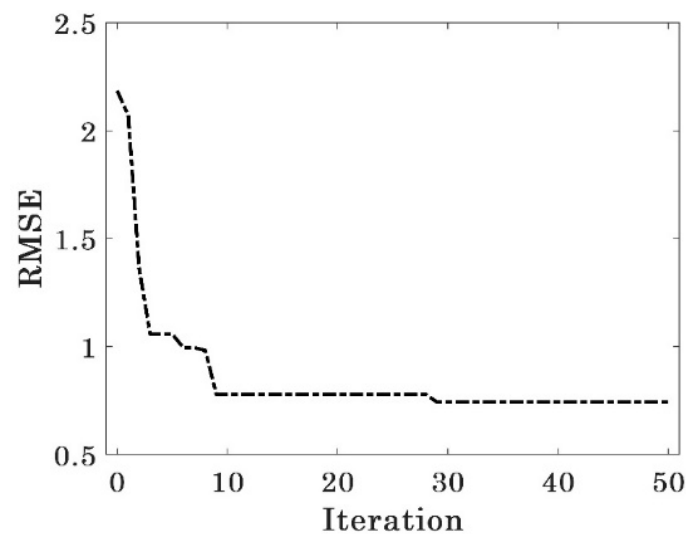


Figure 9. RMSE values with the increase in the iteration times.

5.3. Evaluation of the Model

In the field of artificial intelligence, it is necessary to evaluate the established model after it is established to judge the accuracy of the established artificial intelligence model. This study verifies the accuracy of the PSO and RF hybrid artificial intelligence technology in predicting the permeability of permeable concrete by comparing the predicted value and the actual value of the training set and the test set. The comparison between the predicted value and the actual value of the permeability of permeable concrete in the training set and the test set is shown in Figure 9, and the horizontal line represents the error. It can be observed in Figure 10 that the predicted values of the permeability of permeable concrete in the training set and the test set have a high consistency with the actual values, which proves that the hybrid machine learning technique of PSO and RF proposed in this paper has a good prediction effect on the permeability of permeable concrete.

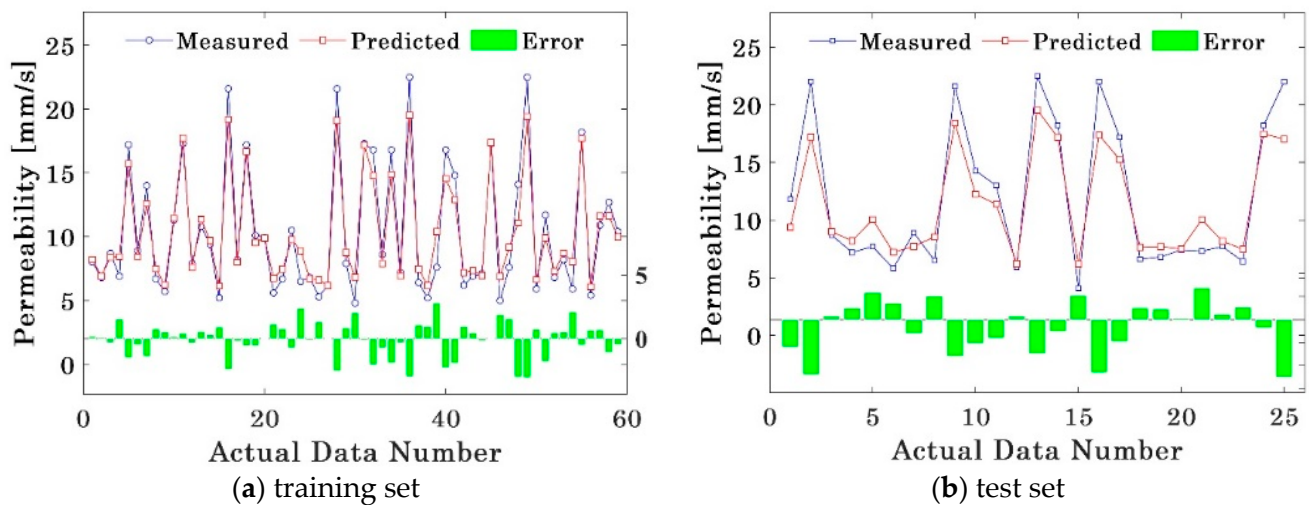


Figure 10. Comparison of the predicted value with the actual value.

Figure 11 more intuitively shows the comparison between the predicted value and the actual value of the permeability of permeable concrete in the training set and the test set, as well as the R value and the RSME value corresponding to the training set and the test set. It can be seen in Figure 10 that the permeability of permeable concrete in both the training set and the test set is concentrated in 0–20mm/s. Most of the predicted values have a high consistency with the actual values, and only a few points have a large error, which will not affect the overall prediction effect of the model on the permeability of permeable concrete. It can also be seen in Figure 11 that the R values of the training set and the test set were 0.978 and 0.9734, respectively, and the RME values were 1.3638 and 2.3246, respectively, that is, the R values of the training set and the test set were very high, and the RME values were very low (it should be noted that the standard deviation of the training set and the test set were 5.30 and 5.74, respectively). It is proven again that the hybrid artificial intelligence technology of particle swarm optimization and radio frequency proposed in this paper can predict the permeability of permeable concrete with high precision. In conclusion, the model can provide a reliable prediction for the possible plugging behavior of permeable concrete and its development trend. The model provides a reference for the maintenance engineers of permeable pavement to understand the blocking behavior, propose a reasonable maintenance time, and determine the corresponding maintenance strategies.

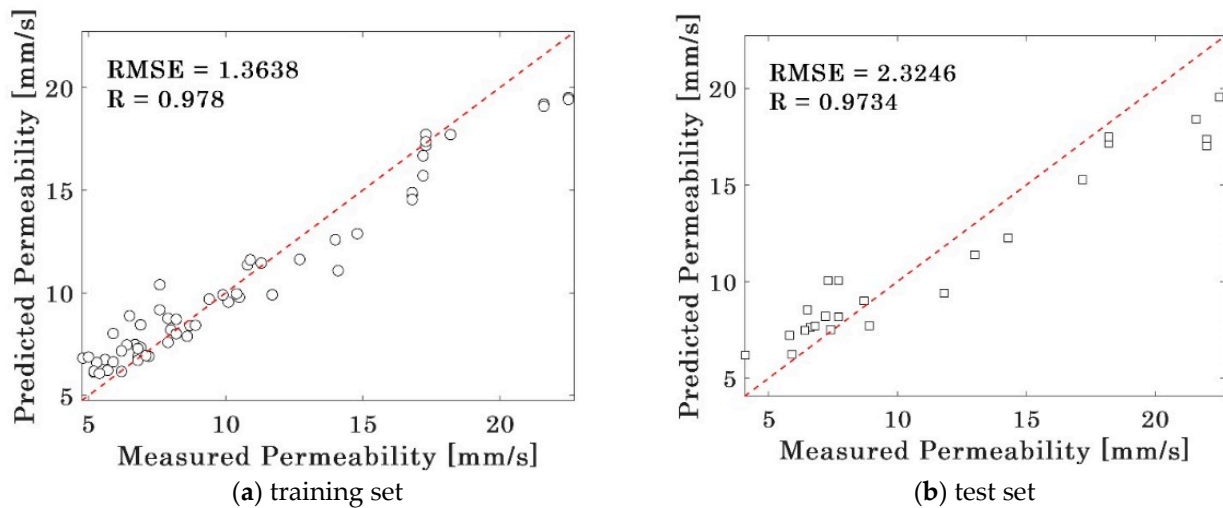


Figure 11. Consistency analysis of the predicted value and the actual value.

To understand the predictive results of the clogging behavior with other research and standard codes, an in-depth comparison was conducted with the previous studies [65,66]. Figure 12 demonstrates the comparison between the proposed model and the previous studies (one is a physical-based prediction model considering the clogging behavior [67,68]; the other is a hybrid machine learning algorithm based on a PSO-SVM model [52]). It can be observed that the prediction results based on the machine learning models are better than the physical model. Also, the hybrid algorithm-based model proposed in this study achieved better results than the PSO-SVM model used in a previous study. This is because the proposed physical models are more based on idealized assumptions. For example, the connected pore is assumed to be an equally thick permeable pipe [67,68], or the porosity of the concrete specimens is assumed to be consistent in different sections [67,68]. It is easy for the physical model to be inconsistent with the actual seepage when predicting the permeation decay behavior of pervious concrete, which leads to the low prediction reliability of the physical model. Also, it can be indicated in the figure that the PSO model shows higher reliability when predicting the permeability attenuation behavior of pervious concrete by tuning the hyperparameters of the RF model compared with the SVM model. This will provide a basis for future engineers to predict the permeability attenuation behavior of pervious concrete using artificial intelligence methods.

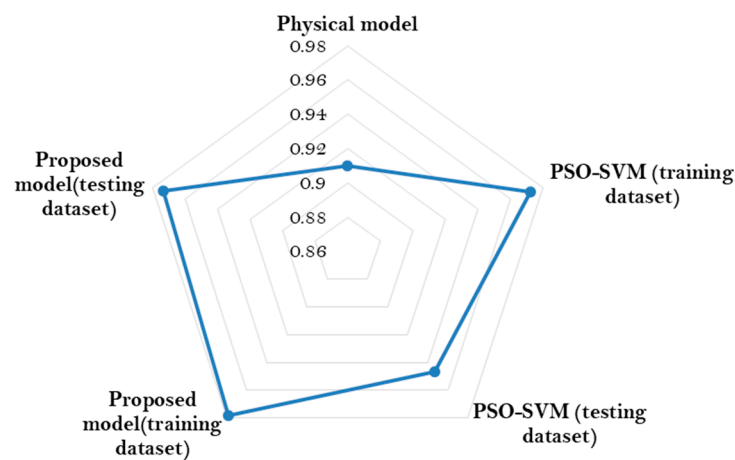


Figure 12. Comparison between the physical model, the PSO-SVM model, and the proposed model in this study.

6. Conclusions

Permeable concrete is a type of multifunctional building material that can improve ecological circulation, protect the ecological environment, and solve the negative influence of modern urban construction on the urban ecological environment. Permeable concrete has many functions, such as water permeability, skid resistance, sound absorption, and noise reduction, among which water permeability is the most important property. However, as the service time of permeable concrete increases, the water permeability of permeable concrete gradually decreases, so it is a great challenge for engineers to design permeable concrete with a strong water permeability. In this study, the PSO and RF hybrid artificial intelligence techniques were proposed to predict the water permeability of permeable concrete. The study drew the following conclusions:

With the increase in the number of iterations, the RMSE value obtained using PSO and 10x cross-validation was at least 0.7. This indicates that the RF model has a good tuning effect for predicting the permeability of pervious concrete.

The increase in the proportion of the small aggregate size harms the permeability of permeable concrete, the increase in the concrete thickness is beneficial to improve the permeability of the permeable concrete, and the increase in blocked particle size will significantly reduce the permeability of the permeable concrete.

Comparing the predicted and actual values of pervious concrete in both the training set and the test set, it was observed that the disparity between the predicted and actual values in both sets was less than 5. The R value and the RMSE value were analyzed for both sets. The RMSE value for the training group was found to be 1.3638, while for the test group it was 2.3246. Additionally, the R values obtained for the training group and the test group were determined to be 0.978 and 0.9734, respectively. Hence, this study effectively demonstrated that the proposed mixed artificial intelligence technology combining PSO and RF can provide improved predictions of water permeability in pervious concrete.

According to the RMSE value of 2.2346 and R value of 0.9734 of the test set, the model demonstrated the capability to reliably predict potential plugging behavior and developmental trends in pervious concrete. Simultaneously, the model offer valuable insights into plugging behavior for the maintenance engineers working with permeable pavement, enabling them to propose appropriate maintenance schedules, determine corresponding measures, and provide a point of reference.

In this study, the influences of the different aggregate compositions, the thickness of the permeable pavement, and the size of clogging particles on the clogging behavior were considered. However, it should be noted that there may be more factors affecting the clogging behavior of permeable concrete (such as the water–cement ratio and the content of additives). Therefore, more possible factors should be considered in future studies to achieve the prediction of clogging behavior. The training and testing datasets were also collected from the same study. Regarding future development, the prediction results should be compared with the other studies to achieve a comprehensive prediction.

Author Contributions: Conceptualization, F.Z. and J.H.; Methodology, F.Z., X.W. and J.H.; Software, F.Z. and J.H.; Validation, X.W.; Data curation, X.W.; Writing—original draft, F.Z., Y.L. and J.H.; Writing—review & editing, X.W., Y.L. and J.H.; Supervision, Y.L. All authors have read and agreed to the published version of the manuscript.

Funding: This research received no external funding.

Data Availability Statement: The datasets generated during and/or analyzed during the current study are available from the corresponding author on reasonable request.

Acknowledgments: This research was funded by the National Natural Science Foundation of China (Grant No. 52108426), the Faculty Start-up Grant of China University of Mining and Technology (Grant No. 102520282), and the Natural Science Foundation of Jiangsu Province (Grant No. BK20210513).

Conflicts of Interest: The authors declare no conflict of interest.

References

1. Wang, Q.; Cheng, T.; Lu, Y.; Liu, H.; Zhang, R.; Huang, J. Underground Mine Safety and Health: A Hybrid MEREC‐CoCoSo System for the Selection of Best Sensor. *Sensors* **2024**, *24*, 1285. [[CrossRef](#)] [[PubMed](#)]
2. Zhang, J.; Wang, R.; Lu, Y.; Huang, J. Prediction of Compressive Strength of Geopolymer Concrete Landscape Design: Application of the Novel Hybrid RF‐GWO‐XGBoost Algorithm. *Buildings* **2024**, *14*, 591. [[CrossRef](#)]
3. Tan, Y.; Zhu, Y.; Xiao, H. Evaluation of the Hydraulic, Physical, and Mechanical Properties of Pervious Concrete Using Iron Tailings as Coarse Aggregates. *Appl. Sci.* **2020**, *10*, 2691. [[CrossRef](#)]
4. Huang, J.D.; Zhang, J.; Li, X.; Qiao, Y.N.; Zhang, R.H.; Kumar, G.S. Investigating the effects of ensemble and weight optimization approaches on neural networks' performance to estimate the dynamic modulus of asphalt concrete. *Road Mater. Pavement Des.* **2023**, *24*, 1939–1959. [[CrossRef](#)]
5. Seeni, B.S.; Madasamy, M. Factors influencing performance of pervious concrete. *Gradevinar* **2021**, *73*, 1017–1030. [[CrossRef](#)]
6. Khosravani, M.R.; Nasiri, S.; Anders, D.; Weinberg, K. Prediction of dynamic properties of ultra-high performance concrete by an artificial intelligence approach. *Adv. Eng. Softw.* **2019**, *127*, 51–58. [[CrossRef](#)]
7. Zhou, H.; Li, H.; Abdelhady, A.; Liang, X.; Wang, H.; Yang, B. Experimental investigation on the effect of pore characteristics on clogging risk of pervious concrete based on CT scanning. *Constr. Build. Mater.* **2019**, *212*, 130–139. [[CrossRef](#)]
8. Zhong, R.; Xu, M.; Netto, R.V.; Wille, K. Influence of pore tortuosity on hydraulic conductivity of pervious concrete: Characterization and modeling. *Constr. Build. Mater.* **2016**, *125*, 1158–1168. [[CrossRef](#)]
9. Adamu, M.; Ayeni, K.O.; Haruna, S.I.; Mansour, Y.E.-H.I.; Haruna, S. Durability performance of pervious concrete containing rice husk ash and calcium carbide: A response surface methodology approach. *Case Stud. Constr. Mater.* **2021**, *14*, e00547. [[CrossRef](#)]
10. Wang, R.; Zhang, J.; Lu, Y.; Ren, S.; Huang, J. Towards a Reliable Design of Geopolymer Concrete for Green Landscapes: A Comparative Study of Tree-Based and Regression-Based Models. *Buildings* **2024**, *14*, 615. [[CrossRef](#)]
11. Huang, J.D.; Xue, J.H. Optimization of SVR functions for flyrock evaluation in mine blasting operations. *Environ. Earth Sci.* **2022**, *81*, 434. [[CrossRef](#)]
12. Liu, H.; Luo, G.; Zhou, P.; Wei, H.; Li, W.; Yu, D. Flexural-Fatigue Properties of Sustainable Pervious Concrete Pavement Material Containing Ground Tire Rubber and Silica Fume. *Sustainability* **2019**, *11*, 4467. [[CrossRef](#)]
13. Soundararajan, E.K.; Vaiyapuri, R. Geopolymer binder for pervious concrete. *Gradevinar* **2021**, *73*, 209–218. [[CrossRef](#)]
14. Liu, R.; Chi, Y.; Chen, S.; Jiang, Q.; Meng, X.; Wu, K.; Li, S. Influence of Pore Structure Characteristics on the Mechanical and Durability Behavior of Pervious Concrete Material Based on Image Analysis. *Int. J. Concr. Struct. Mater.* **2020**, *14*, 29. [[CrossRef](#)]
15. Adil, G.; Kevern, J.T.; Mann, D. Influence of silica fume on mechanical and durability of pervious concrete. *Constr. Build. Mater.* **2020**, *247*, 118453. [[CrossRef](#)]
16. Arifi, E.; Cahya, E.N.; Setyowulan, D. The Influence of Various Materials to the Void Ratio of Pervious Concrete. In Proceedings of the 3rd International Conference of Water Resources Development and Environmental Protection (ICWRDEP), Malang, Indonesia, 12–13 October 2019.
17. Liu, H.; Luo, G.; Wang, L.; Wang, W.; Li, W.; Gong, Y. Laboratory Evaluation of Eco-Friendly Pervious Concrete Pavement Material Containing Silica Fume. *Appl. Sci.* **2019**, *9*, 73. [[CrossRef](#)]
18. Nghopok, C.; Sata, V.; Satiennam, T.; Klungboonkrong, P.; Chindaprasirt, P. Mechanical Properties, Thermal Conductivity, and Sound Absorption of Pervious Concrete Containing Recycled Concrete and Bottom Ash Aggregates. *KSCE J. Civ. Eng.* **2018**, *22*, 1369–1376. [[CrossRef](#)]
19. Huang, J.D.; Zhang, Y.; Sun, Y.T.; Ren, J.L.; Zhao, Z.D.; Zhang, J.F. Evaluation of pore size distribution and permeability reduction behavior in pervious concrete. *Constr. Build. Mater.* **2021**, *290*, 123228. [[CrossRef](#)]
20. Tang, C.-W.; Cheng, C.-K.; Tsai, C.-Y. Mix Design and Mechanical Properties of High-Performance Pervious Concrete. *Materials* **2019**, *12*, 2577. [[CrossRef](#)]
21. Xie, X.; Zhang, T.; Wang, C.; Yang, Y.; Bogush, A.; Khayrulina, E.; Huang, Z.; Wei, J.; Yu, Q. Mixture proportion design of pervious concrete based on the relationships between fundamental properties and skeleton structures. *Cem. Concr. Compos.* **2020**, *113*, 103693. [[CrossRef](#)]
22. Cai, J.; Du, G.; Xia, H.; Sun, C. Model tests on pervious concrete pile and impervious concrete pile composite foundation. In Proceedings of the 8th Asia Conference on Mechanical and Materials Engineering (ACMME), Singapore, 11–14 June 2020.
23. Cai, J.; Chen, J.-g.; Shi, J.; Tian, Q.; Xu, G.; Du, Y. A novel approach to evaluate the clogging resistance of pervious concrete. *Case Stud. Constr. Mater.* **2022**, *16*, e00864. [[CrossRef](#)]
24. Yang, X.; Liu, J.; Li, H.; Ren, Q. Performance and ITZ of pervious concrete modified by vinyl acetate and ethylene copolymer dispersible powder. *Constr. Build. Mater.* **2020**, *235*, 117532. [[CrossRef](#)]
25. Ipek, S.; Diri, A.; Mermerdas, K. Recycling the low-density polyethylene pellets in the pervious concrete production. *J. Mater. Cycles Waste Manag.* **2021**, *23*, 272–287. [[CrossRef](#)]
26. Liu, H.; Luo, G.; Wang, L.; Gong, Y. Strength Time-Varying and Freeze-Thaw Durability of Sustainable Pervious Concrete Pavement Material Containing Waste Fly Ash. *Sustainability* **2019**, *11*, 176. [[CrossRef](#)]
27. Li, K.; Long, Y.; Wang, H.; Wang, Y.-F. Modeling and Sensitivity Analysis of Concrete Creep with Machine Learning Methods. *J. Mater. Civ. Eng.* **2021**, *33*, 04021206. [[CrossRef](#)]
28. Nazari, A.; Hajjiallahyari, H.; Rahimi, A.; Khanmohammadi, H.; Amini, M. Prediction compressive strength of Portland cement-based geopolymers by artificial neural networks. *Neural Comput. Appl.* **2019**, *31*, 733–741. [[CrossRef](#)]

29. Haruna, S.; Malami, S.I.; Adamu, M.; Usman, A.; Farouk, A.; Ali, S.I.A.; Abba, S. Compressive strength of self-compacting concrete modified with rice husk ash and calcium carbide waste modeling: A feasibility of emerging emotional intelligent model (EANN) versus traditional FFNN. *Arab. J. Sci. Eng.* **2021**, *46*, 11207–11222. [[CrossRef](#)]
30. Adamu, M.; Haruna, S.; Malami, S.I.; Ibrahim, M.; Abba, S.; Ibrahim, Y.E. Prediction of compressive strength of concrete incorporated with jujube seed as partial replacement of coarse aggregate: A feasibility of Hammerstein–Wiener model versus support vector machine. *Model. Earth Syst. Environ.* **2021**, *8*, 3435–3445. [[CrossRef](#)]
31. AlHamaydeh, M.; Markou, G.; Bakas, N.; Papadrakakis, M. AI-based shear capacity of FRP-reinforced concrete deep beams without stirrups. *Eng. Struct.* **2022**, *264*, 114441. [[CrossRef](#)]
32. Koopialipoor, M.; Tootoonchi, H.; Armaghani, D.J.; Mohamad, E.T.; Hedayat, A. Application of deep neural networks in predicting the penetration rate of tunnel boring machines. *Bull. Eng. Geol. Environ.* **2019**, *78*, 6347–6360. [[CrossRef](#)]
33. Hasanipanah, M.; Armaghani, D.J.; Amnieh, H.B.; Abd Majid, M.Z.; Tahir, M.M. Application of PSO to develop a powerful equation for prediction of flyrock due to blasting. *Neural Comput. Appl.* **2017**, *28*, 1043–1050. [[CrossRef](#)]
34. Armaghani, D.J.; Koopialipoor, M.; Marto, A.; Yagiz, S. Application of several optimization techniques for estimating TBM advance rate in granitic rocks. *J. Rock Mech. Geotech. Eng.* **2019**, *11*, 779–789. [[CrossRef](#)]
35. Koopialipoor, M.; Armaghani, D.J.; Hedayat, A.; Marto, A.; Gordan, B. Applying various hybrid intelligent systems to evaluate and predict slope stability under static and dynamic conditions. *Soft Comput.* **2019**, *23*, 5913–5929. [[CrossRef](#)]
36. Armaghani, D.J.; Hasanipanah, M.; Mohamad, E.T. A combination of the ICA-ANN model to predict air-overpressure resulting from blasting. *Eng. Comput.* **2016**, *32*, 155–171. [[CrossRef](#)]
37. Armaghani, D.J.; Asteris, P.G. A comparative study of ANN and ANFIS models for the prediction of cement-based mortar materials compressive strength. *Neural Comput. Appl.* **2021**, *33*, 4501–4532. [[CrossRef](#)]
38. Armaghani, D.J.; Raja, R.S.N.S.B.; Faizi, K.; Rashid, A.S.A. Developing a hybrid PSO–ANN model for estimating the ultimate bearing capacity of rock-socketed piles. *Neural Comput. Appl.* **2017**, *28*, 391–405. [[CrossRef](#)]
39. Koopialipoor, M.; Ghaleini, E.N.; Tootoonchi, H.; Armaghani, D.J.; Haghghi, M.; Hedayat, A. Developing a new intelligent technique to predict overbreak in tunnels using an artificial bee colony-based ANN. *Environ. Earth Sci.* **2019**, *78*, 1–14. [[CrossRef](#)]
40. Koopialipoor, M.; Fahimifar, A.; Ghaleini, E.N.; Momenzadeh, M.; Armaghani, D.J. Development of a new hybrid ANN for solving a geotechnical problem related to tunnel boring machine performance. *Eng. Comput.* **2020**, *36*, 345–357. [[CrossRef](#)]
41. Armaghani, D.J.; Mohamad, E.T.; Narayanasamy, M.S.; Narita, N.; Yagiz, S. Development of hybrid intelligent models for predicting TBM penetration rate in hard rock condition. *Tunn. Undergr. Space Technol.* **2017**, *63*, 29–43. [[CrossRef](#)]
42. Cai, M.; Koopialipoor, M.; Armaghani, D.J.; Thai Pham, B. Evaluating slope deformation of earth dams due to earthquake shaking using MARS and GMDH techniques. *Appl. Sci.* **2020**, *10*, 1486. [[CrossRef](#)]
43. Hasanipanah, M.; Monjezi, M.; Shahnazar, A.; Armaghani, D.J.; Farazmand, A. Feasibility of indirect determination of blast induced ground vibration based on support vector machine. *Measurement* **2015**, *75*, 289–297. [[CrossRef](#)]
44. Hasanipanah, M.; Noorian-Bidgoli, M.; Armaghani, D.J.; Khamesi, H. Feasibility of PSO-ANN model for predicting surface settlement caused by tunneling. *Eng. Comput.* **2016**, *32*, 705–715. [[CrossRef](#)]
45. Hajihassani, M.; Armaghani, D.J.; Marto, A.; Mohamad, E.T. Ground vibration prediction in quarry blasting through an artificial neural network optimized by imperialist competitive algorithm. *Bull. Eng. Geol. Environ.* **2015**, *74*, 873–886. [[CrossRef](#)]
46. Huang, J.; Li, X.; Zhang, J.; Sun, Y.; Ren, J. Determining the Rayleigh damping parameters of flexible pavements for finite element modeling. *J. Vib. Control* **2022**, *28*, 3181–3194. [[CrossRef](#)]
47. Imran, H.; Al-Abdaly, N.M.; Shamsa, M.H.; Shatnawi, A.; Ibrahim, M.; Ostrowski, K.A. Development of Prediction Model to Predict the Compressive Strength of Eco-Friendly Concrete Using Multivariate Polynomial Regression Combined with Stepwise Method. *Materials* **2022**, *15*, 317. [[CrossRef](#)] [[PubMed](#)]
48. Han, T.H.; Siddique, A.; Khayat, K.; Huang, J.; Kumar, A. An ensemble machine learning approach for prediction and optimization of modulus of elasticity of recycled aggregate concrete. *Constr. Build. Mater.* **2020**, *244*, 118271. [[CrossRef](#)]
49. Liu, K.H.; Alam, M.S.; Zhu, J.; Zheng, J.K.; Chi, L. Prediction of carbonation depth for recycled aggregate concrete using ANN hybridized with swarm intelligence algorithms. *Constr. Build. Mater.* **2021**, *301*, 124382. [[CrossRef](#)]
50. Chen, D.; Lv, Z. Artificial intelligence enabled Digital Twins for training autonomous cars. *Internet Things Cyber-Phys. Syst.* **2022**, *2*, 31–41. [[CrossRef](#)]
51. Ashraf, S. A proactive role of IoT devices in building smart cities. *Internet Things Cyber-Phys. Syst.* **2021**, *1*, 8–13. [[CrossRef](#)]
52. Huang, J.; Zhang, J.; Gao, Y. Evaluating the Clogging Behavior of Pervious Concrete (PC) Using the Machine Learning Techniques. *Comput. Model. Eng. Sci.* **2022**, *130*, 805–821. [[CrossRef](#)]
53. Zhu, F.; Wu, X.; Zhou, M.; Sabri, M.M.; Huang, J. Intelligent Design of Building Materials: Development of an AI-Based Method for Cement-Slag Concrete Design. *Materials* **2022**, *15*, 3833. [[CrossRef](#)] [[PubMed](#)]
54. Huang, J.; Zhou, M.; Yuan, H.; Sabri, M.M.S.; Li, X. Prediction of the Compressive Strength for Cement-Based Materials with Metakaolin Based on the Hybrid Machine Learning Method. *Materials* **2022**, *15*, 3500. [[CrossRef](#)] [[PubMed](#)]
55. Xu, W.; Huang, X.; Yang, Z.; Zhou, M.; Huang, J. Developing Hybrid Machine Learning Models to Determine the Dynamic Modulus (E^*) of Asphalt Mixtures Using Parameters in Witczak 1-40D Model: A Comparative Study. *Materials* **2022**, *15*, 1791. [[CrossRef](#)] [[PubMed](#)]
56. Huang, J.; Zhou, M.; Yuan, H.; Sabri, M.M.; Li, X. Towards Sustainable Construction Materials: A Comparative Study of Prediction Models for Green Concrete with Metakaolin. *Buildings* **2022**, *12*, 772. [[CrossRef](#)]

57. Huang, J.D.; Zhou, M.M.; Zhang, J.; Ren, J.L.; Vatin, N.I.; Sabri, M.M.S. The Use of GA and PSO in Evaluating the Shear Strength of Steel Fiber Reinforced Concrete Beams. *KSCE J. Civ. Eng.* **2022**, *26*, 3918–3931. [[CrossRef](#)]
58. Huang, J.D.; Zhou, M.M.; Zhang, J.; Ren, J.L.; Vatin, N.I.; Sabri, M.M.S. Development of a New Stacking Model to Evaluate the Strength Parameters of Concrete Samples in Laboratory. *Iran. J. Sci. Technol.-Trans. Civ. Eng.* **2022**, *46*, 4355–4370. [[CrossRef](#)]
59. Huang, J.; Zhang, J.; Gao, Y. Intelligently predict the rock joint shear strength using the support vector regression and Firefly Algorithm. *Lithosphere* **2021**, *2021*, 2467126. [[CrossRef](#)]
60. Zhu, F.; Wu, X.; Lu, Y.; Huang, J. Strength Estimation and Feature Interaction of Carbon Nanotubes-Modified Concrete Using Artificial Intelligence-Based Boosting Ensembles. *Buildings* **2024**, *14*, 134. [[CrossRef](#)]
61. Huang, J.; Sabri, M.M.; Ulrikh, D.V.; Ahmad, M.; Alsaffar, K.A. Predicting the Compressive Strength of the Cement-Fly Ash–Slag Ternary Concrete Using the Firefly Algorithm (FA) and Random Forest (RF) Hybrid Machine-Learning Method. *Materials* **2022**, *15*, 4193. [[CrossRef](#)]
62. Zhou, J.; Su, Z.L.; Hosseini, S.; Tian, Q.; Lu, Y.J.; Luo, H.; Xu, X.Q.; Chen, C.P.; Huang, J.D. Decision tree models for the estimation of geo-polymer concrete compressive strength. *Math. Biosci. Eng.* **2024**, *21*, 1413–1444. [[CrossRef](#)]
63. Wu, X.; Zhu, F.; Zhou, M.; Sabri, M.M.S.; Huang, J. Intelligent Design of Construction Materials: A Comparative Study of AI Approaches for Predicting the Strength of Concrete with Blast Furnace Slag. *Materials* **2022**, *15*, 4582. [[CrossRef](#)] [[PubMed](#)]
64. Huang, J.; Zhou, M.; Sabri, M.M.S.; Yuan, H. A Novel Neural Computing Model Applied to Estimate the Dynamic Modulus (DM) of Asphalt Mixtures by the Improved Beetle Antennae Search. *Sustainability* **2022**, *14*, 5938. [[CrossRef](#)]
65. Zhu, F.; Wu, X.; Lu, Y.; Huang, J. Strength Reduction Due to Acid Attack in Cement Mortar Containing Waste Eggshell and Glass: A Machine Learning-Based Modeling Study. *Buildings* **2024**, *14*, 225. [[CrossRef](#)]
66. Ji, Z.; Zhou, M.M.; Wang, Q.; Huang, J.D. Predicting the International Roughness Index of JPCP and CRCP Rigid Pavement: A Random Forest (RF) Model Hybridized with Modified Beetle Antennae Search (MBAS) for Higher Accuracy. *CMES-Comput. Model. Eng. Sci.* **2024**, *139*, 1557. [[CrossRef](#)]
67. Wang, R.; Zhang, J.; Lu, Y.; Huang, J. Towards Designing Durable Sculptural Elements: Ensemble Learning in Predicting Compressive Strength of Fiber-Reinforced Nano-Silica Modified Concrete. *Buildings* **2024**, *14*, 396. [[CrossRef](#)]
68. Shi, X.; Chen, S.; Wang, Q.; Lu, Y.; Ren, S.; Huang, J. Mechanical Framework for Geopolymer Gels Construction: An Optimized LSTM Technique to Predict Compressive Strength of Fly Ash-Based Geopolymer Gels Concrete. *Gels* **2024**, *10*, 148. [[CrossRef](#)]

Disclaimer/Publisher’s Note: The statements, opinions and data contained in all publications are solely those of the individual author(s) and contributor(s) and not of MDPI and/or the editor(s). MDPI and/or the editor(s) disclaim responsibility for any injury to people or property resulting from any ideas, methods, instructions or products referred to in the content.